Chapter 31
Transmission Models

The take-off manoeuvre of a vehicle was studied in Sect. 23.9 using a simple model where the inertia of both engine and vehicle were modelled as two flywheels connected to each other by a rigid shaft and a friction clutch. This model can be made more realistic by adding the torsional compliance of the shaft, of the joints and possibly the gear wheels, as well as the rotational inertia of the various elements of the driveline. A model of the whole driveline is thus obtained, with the engine and vehicle modelled as two flywheels located at its ends.

However, the engine shaft is itself a compliant system. Moreover, its piston-connecting rod-crank systems should be modelled as systems with variable inertia in time. At the other end of the driveline, the dynamics of the transmission and the longitudinal dynamics of the vehicle are coupled by the tires, which are themselves compliant in torsion. The longitudinal compliance of the suspensions may affect the dynamics of the driveline and couples with the dynamics of the vehicle, which is in turn coupled with comfort dynamics.

Because many of the parts that may be included in the model of the driveline have a strongly nonlinear behavior, the model must include nonlinearities that prevent frequency domain solutions from being obtained if a high degree of detail is to be considered. In this case only time domain solutions can be obtained.

The mathematical models of the various parts of the transmission, from the engine to the vehicle, will be described in this chapter.

31.1 Coupling Between Comfort and Driveline Vibration

As predictable in a system with many degrees of freedom, the driveline has many vibration modes and natural frequencies. The effects of the various modes are different, and a variety of models may be used for their study.

G. Genta and L. Morello, *The Automotive Chassis*, Mechanical Engineering Series, https://doi.org/10.1007/978-3-030-35709-2_31

The most important mode for comfort is the first mode of the driveline, which usually has a natural frequency not much different from those typical of the comfort modes of the sprung mass related to heave and pitch. In this mode the transmission behaves as a massless torsional spring connecting two large inertias at its ends, those of the engine and the vehicle.

An extremely simple model may be used to study this mode, similar to those used earlier for the take-off manoeuvre, the difference being that the clutch may now be considered as a rigid joint. The natural frequencies of the crankshaft are much higher, and at these low frequencies the engine may be considered as a single moment of inertia.

In all reciprocating engines the driving torque changes in time, with a period depending on the duration of the thermodynamic cycle, lasting two revolutions of the crankshaft (in four-stroke cycle engines, one revolution in two-stroke cycle engines). These frequencies are higher, often much higher, than 10 Hz. The driving torque may be considered as constant at its average value computed over one cycle: The variability of the pressure of the working gases on the piston and the driving torque cannot excite vibration at such a low frequency.

Slower variations of the driving torque, however, such as those due to manipulation of the accelerator pedal, may have an important role in exciting low frequency vibration. A typical case is that of a manoeuvre usually called *tip-in, tip-out*: The driver pushes suddenly on the accelerator pedal while the vehicle is travelling at a constant speed, usually low, causing a driving torque step. The step increase of the driving torque may be followed by an equally sudden release of the accelerator pedal.

Some experimental results obtained during a tip-in, tip-out manoeuvre are shown in Fig. 31.1. The vehicle travels on a straight road at a given speed (in the figure, at a speed corresponding to an engine speed of about 1,500 rpm in top gear) and, when all parameters are constant, the accelerator pedal is pushed fully down. When the engine speed has increased by about 500 rpm the accelerator is fully released until the previous speed has again been attained. This manoeuvre is repeated several times, at different initial speeds and with different gears engaged. One of the cycles is shown in the figure; its duration is about 8 s.

The results shown were filtered with a low-pass filter removing all frequencies higher than 25 Hz to make all phenomena occurring in the frequency range from 0 to 10 Hz more apparent. As can be seen, the vehicle velocity shows strong oscillations, causing longitudinal accelerations that were measured at two points important for comfort: The attachment points of the seat and its back. By analyzing the results it is possible to show that when the engine is accelerating the forced oscillations have a frequency of about 4 Hz, while when the vehicle slows their frequency is 3 Hz. This difference can be explained by the nonlinearity of some elements, such as the damper springs of the clutch disk, that perform more stiffly when heavily loaded in torsion.

As is common for step inputs, all frequencies of the system are in this way excited, particularly low frequencies, because the response of the engine is not immediate and smooths out what in theory should be a true step. The vehicle therefore does not accelerate (or decelerate) smoothly and torsional vibration of the driveline causes

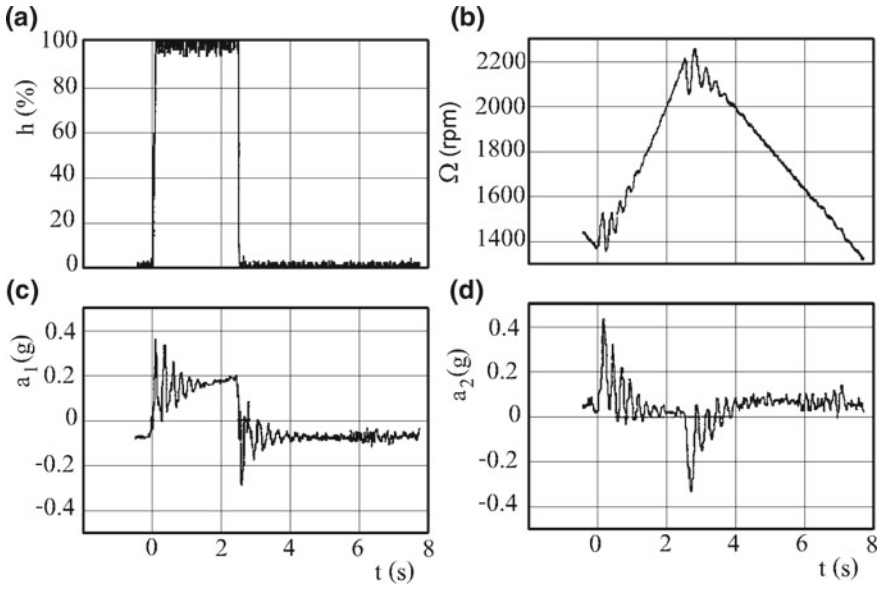

Fig. 31.1 Experimental results obtained in a tip-in, tip-out manoeuver. **a** throttle opening; **b** engine speed; **c** longitudinal acceleration measured at the attachment opoints of the seat; **d** longitudinal acceleration at the back of the seat

longitudinal oscillations of the whole vehicle, with vertical motions of the sprung and unsprung masses.

This manoeuvre may be performed at different speeds and in different ways, but the oscillations produced by it strongly reduce comfort, making it an important issue in vehicle testing. If problems appear, adequate correction must be introduced, usually by increasing the torsional natural frequencies of the driveline or its damping. A provision that was recently found to be quite effective is the use of a flywheel damper with two masses, as shown in Part II. The engine flywheel is divided into two parts, connected to each other by a low stiffness spring and adequate damping. Because the torsional oscillations of the transmission are triggered by manipulation of the accelerator, an effective solution is to modify the throttle control of the engine so that sudden increases of the engine torque are avoided. This is simple if a *by wire* engine control is used, because it is sufficient to introduce a smoother control algorithm into the system.

Apart from low frequency vibration, higher frequency vibration caused by the torsional vibration of the crankshaft of the engine or the gearbox, is possible. Its effect is to increase the noise produced by the gearbox (in jargon, *rattle*) and to cause fatigue problems in the crankshaft, the shafts of the gearbox and gearwheels. When this occurs, the useful provisions are, besides the use of a twin-mass flywheel,

those typical of torsional vibration, i.e. inserting in the engine and possibly in the driveline suitable torsional dampers or compliant joints that uncouple the vibration of the various parts of the system.

31.2 Dynamic Model of the Engine

Almost all vehicles presently on the road are propelled by a reciprocating internal combustion engine. Machines containing reciprocating elements have some peculiar dynamic problems.

Most reciprocating machines, and practically all those used in the automotive industry, are based on a crank mechanism, often in the form of a crankshaft with several connecting rods and reciprocating elements. Such devices cannot, in general, be exactly balanced: The inertial forces they exert on the structure of the vehicle constitute a system of forces whose resultant is not insignificant and is variable in time. The geometric configuration of the system created by the crankshaft, the connecting rods, and the reciprocating elements can be quite complex. Crankshafts not only do not possess axial symmetry but often lack symmetry planes.

In these conditions, uncoupling among axial, torsional, and flexural behavior is not possible, in anything other than a rough approximation, and vibration modes become quite complicated. The external forces acting on the elements of reciprocating machines are usually variable in time, often following periodic laws, as the forces exerted by hot gases on the pistons of reciprocating internal-combustion engines demonstrate. Their period is equal to the rotation period in two-stroke cycle engines and is twice the rotation period in four-stroke cycle engines. Their periodic time histories are not harmonic but, once harmonic analysis has been performed, they may be considered as the sum of many harmonic components whose frequencies are usually multiples, by a whole number or a rational fraction, of the rotational speed of the machine. There may be many possibilities of resonance between these forcing functions and the natural frequencies of the system.

In general, the most dangerous vibrations are linked to modes that are essentially torsional. These couple with the modes of the driveline and the longitudinal dynamics of the vehicle.

31.2.1 Equivalent System for a Crank Mechanism

The traditional approach to the study of torsional vibrations in reciprocating machines is based on the reduction of the actual system made of crankshafts, connecting rods, and reciprocating elements to an equivalent system. The latter is usually modeled

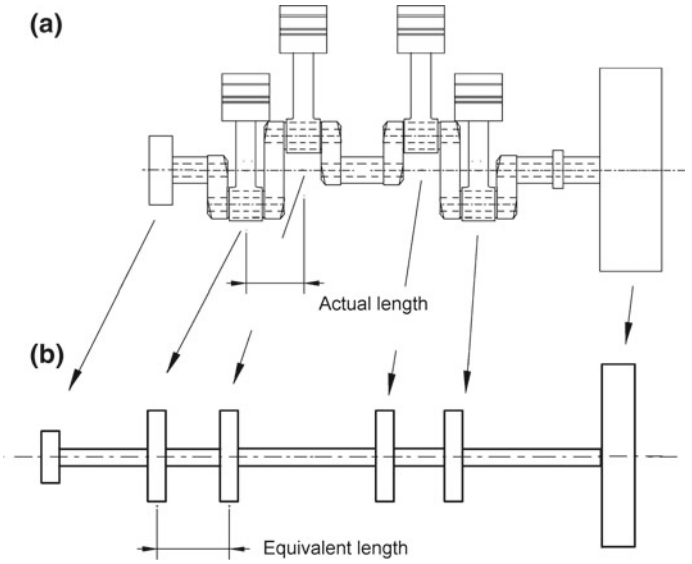

Fig. 31.2 Sketch of the crankshaft: **a** actual system; **b** equivalent system, lumped-parameters model

as a lumped-parameters system whose torsional behavior can be studied separately[1] (Fig. 31.2).

Consider the crank mechanism sketched in Fig. 31.3. It is made of a disc, with a crankpin in B on which the connecting rod PB, whose center of mass is G, is articulated. The reciprocating parts of the machine are articulated to the connecting rod in P. The actual position of the center of mass of the reciprocating elements, which may include the piston as well as the crosshead and other parts, is not important in the analysis; in the following study this point will be assumed to be located directly in P. The axis of the cylinder, i.e., the line of motion of point P, does not necessarily pass through the axis of the shaft; the offset d will, however, be assumed to be small. Let J_d, J_b, m_b, and m_p be the moment of inertia of the disc that constitutes the crank, the moment of inertia of the connecting rod (about its center of gravity G) and the masses of the connecting rod and of the reciprocating parts, respectively.

The coordinates of points B, G, and P can be expressed in the reference frame Oxy, shown in Fig. 31.3 as functions of the crank angle θ, as

$$(\overline{\text{B-O}}) = \left\{ \begin{array}{l} r\cos(\theta) \\ r\sin(\theta) \end{array} \right\}, \qquad (\overline{\text{G-O}}) = \left\{ \begin{array}{l} r\cos(\theta) + a\cos(\gamma) \\ r\sin(\theta) - a\sin(\gamma) \end{array} \right\}, \tag{31.1}$$

[1] Torsional dynamics of reciprocating machinery is dealt with in many texts on vibration dynamics, like G. Genta, *Vibration of Structures and Machines*, Springer, New York, 1998. For a detailed study, specific texts on the subject can be found, such as E.J. Nestorides, *A handbook on torsional vibration*, Cambridge Univ. Press, 1958; K.E. Wilson, *Torsional vibration problems*, Chapman & Hall, 1963.

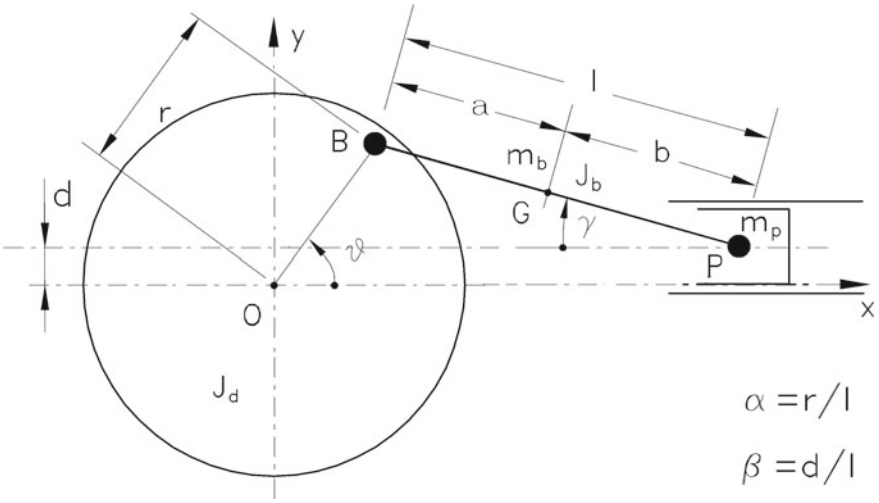

Fig. 31.3 Sketch of the crank mechanism

$$(\overline{\text{P-O}}) = \left\{ \begin{matrix} r\cos(\theta) + l\cos(\gamma) \\ d \end{matrix} \right\}.$$

Angle γ is linked to angle θ by the equation

$$r\sin(\theta) = d + l\sin(\gamma), \tag{31.2}$$

i.e.

$$\sin(\gamma) = \alpha\sin(\theta) - \beta,$$

where

$$\alpha = \frac{r}{l}, \beta = \frac{d}{l}.$$

Ratios α and β are expressed by numbers smaller than 1, and in practice they are quite small; usually $\alpha \leq 0.3$ and $\beta = 0$.

Remark 31.1 In the case of an ideal crank mechanism with an infinitely long connecting rod ($\alpha = 0$), with the axis of the cylinder passing through the axis of the crank ($\beta = 0$), the motion of the reciprocating masses is harmonic when the crank speed is constant.

Because $\dot{\theta}$ is the angular velocity of the crank, its kinetic energy is simply

$$\mathcal{T}_d = \frac{1}{2} J_d \dot{\theta}^2. \tag{31.3}$$

The speed of the reciprocating masses can be easily obtained by differentiating the third equation (31.1) with respect to time and obtaining the expression for $\dot{\gamma}$ from Eq. (31.2):

$$V_p = -r\dot{\theta}\sin(\theta) - l\dot{\gamma}\sin(\gamma) = -r\dot{\theta}\left[\left(1 + \alpha\frac{\cos(\theta)}{\cos(\gamma)}\right)\sin(\theta) - \beta\frac{\cos(\theta)}{\cos(\gamma)}\right]. \tag{31.4}$$

The kinetic energy of the reciprocating masses is

$$\mathcal{T}_p = \frac{1}{2}m_p r^2\dot{\theta}^2 f_1(\theta), \tag{31.5}$$

where

$$f_1(\theta) = \left[\sin(\theta) + \alpha\frac{\sin(2\theta)}{2\cos(\gamma)} - \beta\frac{\cos(\theta)}{\cos(\gamma)}\right]^2.$$

Instead of computing the kinetic energy of the connecting rod by writing the velocity of its center of gravity G, it is customary to replace the rod with a system made of two masses m_1 and m_2, located at the crankpin B and the wrist pin P, respectively, and a moment of inertia J_0. To simulate the connecting rod correctly, such a system must have the same total mass, moment of inertia, and center of mass position. These three conditions produce three equations yielding the following values for m_1, m_2, and J_0:

$$\begin{gathered} m_1 = m_b\frac{b}{l}\quad , \qquad m_2 = m_b\frac{a}{l}\quad , \\ J_0 = J_b - (m_1a^2 + m_2b^2) = J_b - m_bab\,. \end{gathered} \tag{31.6}$$

Generally speaking, the moment of inertia of masses m_1 and m_2 is greater than the actual moment of inertia of the connecting rod and, consequently, the term J_0 is negative. The kinetic energy of mass m_1 can be computed simply by adding a moment of inertia m_1r^2 to that of the crank.

Remark 31.2 The negative moment of inertia has no physical meaning in itself: The minus sign indicates that it is simply a term that must be subtracted in the expression of the kinetic energy.

Similarly, the kinetic energy of mass m_2 can be accounted for by adding m_2 to the reciprocating masses. The effect of the moment of inertia J_0 can be easily computed

$$\mathcal{T}_{J_0} = \frac{1}{2}J_0\dot{\gamma}^2 = \frac{1}{2}J_0\dot{\theta}^2 f_2(\theta), \tag{31.7}$$

where

$$f_2(\theta) = \alpha^2\left[\frac{\cos(\theta)}{\cos(\gamma)}\right]^2.$$

The total kinetic energy of the system shown in Fig. 31.3 is, consequently,

$$\mathcal{T} = \frac{1}{2}\dot{\theta}^2 \left[J_d + m_1 r^2 + (m_2 + m_p) r^2 f_1(\theta) + J_0 f_2(\theta) \right] = \frac{1}{2} J_{eq}(\theta) \dot{\theta}^2 . \tag{31.8}$$

It is now clear that the whole system can be modeled, from the viewpoint of kinetic energy, by a single moment of inertia variable with the crank angle $J_{eq}(\theta)$, rotating at the angular velocity $\dot{\theta}$.

The equivalent moment of inertia is a periodic function of θ, with a period of 2π.

In the limiting case of $\alpha = \beta = 0$, corresponding to an infinitely long connecting rod (piston moving with harmonic time history), the expressions for $f_1(\theta)$ and $f_2(\theta)$ are particularly simple

$$f_1(\theta) = \sin^2(\theta) = \frac{1 - \cos(2\theta)}{2} \quad , \quad f_2(\theta) = 0 \, . \tag{31.9}$$

In practice, it is impossible to neglect the fact that the length of the connecting rod is finite, even if α is usually not greater than 0.3. At any rate there is no difficulty in expressing J_{eq} through a Fourier series

$$J_{eq} = J_0 + \sum_{i=1}^{n} J_{ci} \cos(i\theta) + \sum_{i=1}^{n} J_{si} \sin(i\theta) \, , \tag{31.10}$$

that is here truncated at the nth harmonics. Coefficients J_0, J_{ci} and J_{si} may be computed numerically without difficulty, by computing the values of functions $f_1(\theta)$ and $f_2(\theta)$ for a number of values of angle θ and then applying one of the standard FFT algorithms. The number of values of $J_{eq}(\theta)$ to be computed depends on the value of n and, if many harmonics are required, 2048 or 4096 values may be needed.

Traditionally, before the numerical computation of the coefficients of the Fourier series became straightforward, explicit expressions of the coefficients were used; these are discussed in several handbooks. The coefficients were expressed as power series in α and β; the number of terms needed depends on how many harmonics must be accounted for. To compute six harmonics, series with terms up to α^4 and β^4 were used.

If the axis of the cylinder passes through the center of the crank ($\beta = 0$), as is usually the case, $f_1(\theta)$ and $f_2(\theta)$ are even functions of θ for symmetry reasons. J_{eq} is then an even function and all coefficients J_{si} vanish. If $\alpha = 0$, the expression of the average equivalent moment of inertia reduces to

$$J_0 = J_d + r^2 \frac{2m_1 + m_2 + m_p}{2} . \tag{31.11}$$

31.2.2 Driving Torque

A moment caused by the pressure of the gases contained in the cylinder $p(t)$ acts upon each crank, varying in time during the working cycle of the engine. Once the pressure $p(t)$ is known, the driving torque acting on the crankshaft can be computed from the virtual work $\delta\mathcal{L}$ performed by that pressure during a virtual displacement δs of the piston. A virtual displacement $\delta\theta$ of the crank corresponds to a displacement δs of the piston; the relationship between them is

$$\delta s = \frac{V_p}{\dot{\theta}}\delta\theta = r\sqrt{f_1(\theta)}\delta\theta \,. \tag{31.12}$$

The corresponding virtual work $\delta\mathcal{L}$ performed by this pressure can be expressed as

$$\delta\mathcal{L} = p(t)A\delta s = p(t)rA\sqrt{f_1(\theta)}\delta\theta, \tag{31.13}$$

where function $f_1(\theta)$ is given by Eq. (31.5) and A is the area of the piston. The generalized force M_m due to the pressure $p(t)$, i.e. the driving torque, is consequently

$$M_m = \frac{d(\delta\mathcal{L})}{d(\delta\theta)} = p(t)rA\sqrt{f_1(\theta)}. \tag{31.14}$$

In the case of two-stroke cycle engines working at constant speed, function $p(t)$ is periodic with a period equal to the time needed to perform one revolution of the crankshaft, i.e. its frequency is equal to the rotational speed Ω of the engine. In the case of four-stroke-cycle internal combustion engines, again assuming constant speed operation, the period of function $p(t)$ is doubled, i.e. its fundamental frequency is equal to $\Omega/2$. Because the generalized force (moment) $M_m(t)$ is periodic, with the same frequency of law $p(t)$, it can be expressed by a trigonometric polynomial, truncated after m harmonic terms

$$M_m(t) = M_0 + \sum_{k=1}^{m} M_{ck}\cos(k\omega' t) + \sum_{k=1}^{m} M_{sk}\sin(k\omega' t)\,, \tag{31.15}$$

where the frequency ω' of the fundamental harmonic is equal to Ω, except in the case of four-stroke-cycle internal-combustion engines, in which

$$\omega' = \frac{\Omega}{2}\,. \tag{31.16}$$

The coefficients of the polynomial may be computed starting from the theoretical or experimental law $p(t)$, and empirical expressions can be found in the literature. In any case, the driving torque depends upon working conditions. It is possible to assume that coefficients M_{ck} and M_{sk} are proportional to the average driving torque

M_0 or to the product of half the capacity of the cylinder (the area of the piston times the crank radius) times the mean indicated pressure.

Angle θ may be used instead of time as an independent variable and the driving torque may be written as

$$M_m(\theta) = M_0 + \sum_{k=1}^{m} M_{ck} \cos(k\theta') + \sum_{k=1}^{m} M_{sk} \sin(k\theta') \,, \tag{31.17}$$

where θ' is equal to θ in two-stroke cycle engines and $\theta/2$ in four-stroke cycle engines.

Remark 31.3 When the engine works at variable speed, it may be assumed that the speed variations are much slower than the phenomena occurring in the combustion chamber. Conditions at variable speed may be approximated by a sequence of constant speed operations at the various speeds.

31.2.3 Forcing Functions on the Cranks of Multicylinder Machines

All motor vehicles other than motorcycles powered by single-cylinder engines are provided with reciprocating engines with a number of cylinders. The most common engine arrangement is in-line, but many engines have opposite cylinders or V arrangements.

In machines with a number of cranks, if the various cranks, reciprocating parts, and working cycles are all equal, the time histories of the moments acting on the various nodes of the equivalent system are all equal but are timed differently. Because each harmonic component of the moment acting on the cranks can be represented as the projection on the real axis of a vector rotating in the Argand plane with constant angular velocity, it is possible to draw, for each harmonic, a plot in which the various vectors acting on the different cranks of the machine are represented. Because, as already stated, the amplitudes of these vectors are equal, the diagram is useful only for comparing the phases of the vectors, which are traditionally plotted with unit amplitude. The phasing of the vectors depends on the geometric characteristics of the machine and, in the case of four-stroke-cycle engines, on the firing order. Such diagrams are usually referred to as *phase angle diagrams*.

Consider, for example, an in-line four-stroke-cycle internal-combustion engine. If the working cycles of the various cylinders are evenly spaced in time, the cranks that subsequently fire must be at an angle of $4\pi/n$ rad, where n is the number of cylinders. In a four-in-line engine, this angle is 180°, and the most common geometric configuration of the crankshaft is that shown in Fig. 31.4a, chosen because it allows the best balancing of inertia forces. In the same figure, the configuration of the crankshaft of a six-in-line engine is also shown.

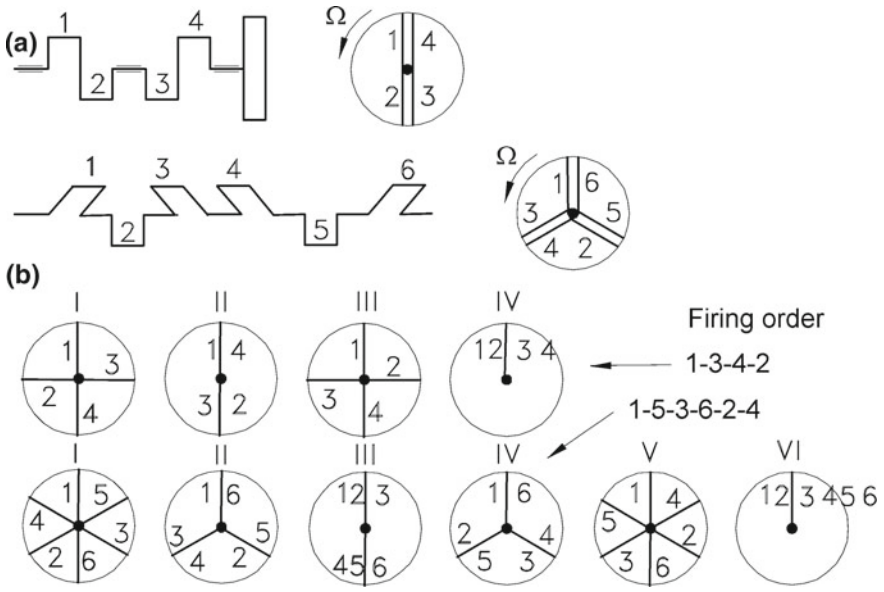

Fig. 31.4 **a** Configuration of the crankshaft and crank angle diagrams for in-line four-stroke-cycle four-and six-cylinder internal combustion engines. In the latter case the configuration shown is just one of the possible choices; **b** phase-angle diagrams for the same engines

In a four-cylinder engine, the possible firing orders are two: 1-2-3-4 and 1-3-4-2. In both cases, it is impossible to prevent two contiguous cylinders from immediately firing one after the other. The phase-angle diagrams for the first four harmonics are plotted in Fig. 31.4b for the second of the two firing orders.

If the order of the harmonic is a whole multiple of the number of cylinders, all rotating vectors are superimposed, i.e. the forcing functions acting on all cranks are all in phase. These harmonics are usually the most dangerous and are often referred to as major harmonics. The phase-angle diagrams for the $(n + i)$-th harmonic coincide with that related to the ith harmonic and, consequently, only the first n phase-angle diagrams are usually plotted.

Remark 31.4 The phase-angle diagrams have been plotted in such a way that they supply the excitation phasing on the various cranks with respect to that acting on a crank chosen as reference, usually the first. Each harmonic then has a phasing with respect to the fundamental harmonic that must be considered when the effects of the various harmonics are added.

The forcing function acting on the jth crank may be approximated by the following series, truncated at the mth harmonic

$$M_{m_j} = \sum_{k=0}^{m} M_{m_k} e^{i\left(k\omega' i + \Phi_{m_k} + \delta_{jk}\right)}, \tag{31.18}$$

where

- M_{m_k} and Φ_{m_k} are the amplitude and phase of the k th harmonic of the driving torque, respectively. With reference to the series (31.15) approximating the driving torque, their values are

$$M_{m_k} = \sqrt{M_{ck}^2 + M_{sk}^2} \text{ and } \Phi_{m_k} = \arctan(M_{ck}/M_{sk}),$$

  respectively.
- δ_{j_k} is the phase of the kth harmonic acting on the jth crank, as obtained from the phase-angle diagram. If the diagram is referred to the first crank, $\delta_{j_k} = 0$ for $j = 1$.

31.2.4 Stiffness of the Crankshaft

From the viewpoint of inertia forces, the cranks and reciprocating elements are equivalent to a number of concentrated flywheels, even if their moments of inertia vary periodically with angle θ. The engine can thus be reduced to a lumped-parameters equivalent system, with the various flywheels connected to each other by straight shafts having an equivalent stiffness that models the actual stiffness of the relevant portion of crankshaft (Fig. 31.2). The various flywheels have a length equal to zero: the lengths of the various parts of the shaft must be contiguous, each starting where the previous one ends. Traditionally, instead of reasoning in terms of equivalent stiffness, the elastic properties of the shaft were computed in terms of equivalent length, assuming that the shaft of the straight equivalent shaft has the same diameter as the relevant part of the actual shaft or, more often, has a conventional value, allowing its length to be computed so that its torsional stiffness is that of the actual shaft.

It is not possible to compute the stiffness by modeling each part of the crank as a simple body (beams loaded in torsion for the journals, beams loaded in bending and torsion for the crankpins, beams loaded in bending for the crank webs, etc.). The complex geometry, the presence of radii, and the low slenderness of the beams make it impossible to resort to such approach.

There are three ways to evaluate the equivalent stiffness:

1. experimental evaluation,
2. use of semi-empirical methods, and
3. numerical modeling, mainly using the FEM.

Experimental evaluation clearly gives the most reliable results, but it cannot be performed at the design stage without additional costs. Moreover, it increases in the time required for dynamic analysis because of the need to build models or prototypes.

Empirical and semi-empirical formulas, allowing at least approximate evaluations to be obtained, have been suggested by many authors and can be found in several handbooks.[2]

Nowadays it is possible to build numerical models of a single crank and to evaluate their static stiffness by numerical methods, mainly the FEM. This is much simpler than the complete numerical simulation of the crankshaft using the same numerical approach. Only one crank (or half, for symmetry) needs to be modelled, assuming all cranks are equal, and the computation reduces to a static evaluation.

Nevertheless, the geometric complexity and uncertainties on how to constrain the mathematical model may make this computation more difficult than it appears.

Remark 31.5 Strictly speaking, the lack of symmetry couples torsional and flexural deformations, and the stiffness of the crankcase and the presence of oil films in the bearings may affect the results.

The equivalent stiffness and equivalent length, computed through any of the mentioned approaches, are linked through the obvious formula

$$k = G\frac{I_p}{l_{eq}}. \tag{31.19}$$

31.2.5 Damping of the System

If the damping present in the engine were mostly caused by the internal damping of the material constituting the crankshaft, there would be no difficulty introducing a proportional damping with modal damping ratio equal for all modes: $\zeta_j = \eta/2$, where η is the loss factor of the material of the crankshaft.

But damping is actually due to many causes, among which friction between moving parts (including that between the piston and the cylinder wall), electromagnetic forces (if an electric motor or generator is driven by the engine), and the presence of fluid in which some rotating parts move, can be important. Neglecting them would lead to a large underestimate of damping. It is usually necessary to resort to experimental results, obtained from machines similar to the one under study, and to empirical or semi-empirical formulas and numerical values reported in the literature.

The damping due to the crank mechanism is usually evaluated by introducing a damping force acting on the crankpin that is proportional to the area of the piston and the velocity of the crankpin. The damping moment acting on the jth crank is

$$M_d(t) = k' A r^2 \,, \tag{31.20}$$

where k' is a coefficient whose dimension is a force multiplied by time and divided by the third power of a length. In S.I. units, it is expressed in Ns/m^3. Values of k'

[2] See, for example, E.J. Nestorides, *A Handbook on Torsional Vibration*, Cambridge Univ. Press, 1958, or W. Ker Wilson, *Torsional Vibration Problems*, Chapman & Hall, 1963.

included in the range between 3,500 and 10,000 Ns/m^3 for in-line aircraft engines and between 15,000 and 1.5×10^6 Ns/m^3 for large internal-combustion engines can be found in the literature.

Remark 31.6 The lower and upper values of these ranges are very different and must be regarded only as indicative values; only experimental results on machines similar to the one under study can be reliable.

The use of Eq. (31.20) leads to the assumption that in each crank there is a viscous damper with damping coefficient equal to

$$c_j = k' A r^2 \,. \tag{31.21}$$

In many cases, it is impossible to prevent the amplitude of torsional vibration from reaching values too large to insure safe operation of the machine or adequate vibrational and acoustic comfort solely by exploiting the damping properties of the system elements.

In such cases, torsional vibration dampers are applied at one end of the crankshaft. They are made of a flywheel (usually referred to as *seismic mass*) whose geometric configuration may draw on a wide variety of types, connected to the shaft by suitable elastic and damping elements.

Almost all torsional vibration dampers can be reduced to the concept of the damped vibration absorber. Without including all possible types, these can be subdivided into three categories: dissipative dampers, damped vibration absorbers, and rotating pendulum vibration absorbers. The latter are seldom used in automotive engines and will not be dealt with here.

A typical dissipative torsional damper used primarily in diesel engines for industrial vehicles is the viscous damper shown in Fig. 31.5a. It is applied to one end of the crankshaft and consists of a flywheel, generally shaped as a ring free to rotate within a casing filled with a high viscosity fluid, for example a silicon-based oil. Damping in this case is of the viscous type, i.e., the drag torque is proportional to the relative angular velocity between the ring and the housing, with the damping coefficient depending on the clearance between the two and on the characteristics of the fluid. The latter are greatly influenced by the fluid temperature. The model for the dynamic study of the system must be modified by adding the moment of inertia of the casing, in the node in which the damper is applied (node 1, Fig. 31.5c), and by adding a new node (node 0 in the same figure) in which the inertia of the ring is located. The two nodes are connected by a viscous damper and a spring with zero stiffness.

A viscous damper of this kind actually lacks stiffness only in static conditions and at very low frequency. The characteristics of the fluid are such that an elastic behavior of increasing strength occurs with increasing frequency, obviously adding to the damping behavior. This means that the torque the damper applies to the shaft depends not only on the relative velocity, but also on the angular displacement. A stiffness, which is a function of the frequency, must be added to the previous model, but this holds only in harmonic, or at least polyharmonic, vibration.

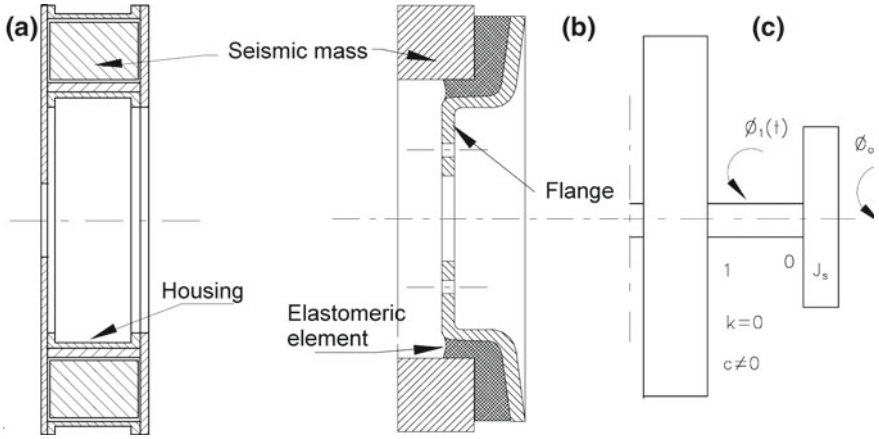

Fig. 31.5 Dissipative torsional vibration damper; **a** viscous damper; **b** elastomeric damper; **c** sketch of the model for the dynamic study

For a first-approximation evaluation of the optimum system damping, it may be assumed that the presence of the damper does not significantly affect the natural frequencies of the system. The above mentioned stiffness may be neglected. Under this assumption, the behavior of the damper may be studied separately, assuming the time history of the motion $\phi_1(t)$ of the node where it is applied. The equation of motion of node 0 is then

$$J_s\ddot{\phi}_0 + c\dot{\phi}_0 = c\dot{\phi}_{1_0} \,. \tag{31.22}$$

Assume that the time history at node 1, where the damper is applied, is harmonic

$$\phi_1(t) = \phi_{1_0} e^{i\omega t} \,.$$

The time history at node 0 is also harmonic

$$\phi_0(t) = \phi_{0_0} e^{i\omega t}$$

although not in phase with the excitation. The response can be computed using the frequency domain equation

$$\left(-J_s\omega^2 + i\omega c\right)\phi_{0_0} = i\omega c\phi_{1_0} \,. \tag{31.23}$$

By separating the real and imaginary parts of the response, it follows that

$$\begin{cases} \Re(\phi_{0_0}) = \phi_{1_0} \dfrac{c^2}{c^2 + J_s^2\omega^2} \,, \\ \Im(\phi_{0_0}) = \phi_{1_0} \dfrac{-cJ_s\omega}{c^2 + J_s^2\omega^2} \,. \end{cases} \tag{31.24}$$

If time $t = 0$ is chosen as the time when the angular displacement ϕ_1 reaches its maximum, i.e. if ϕ_{1_0} is real, the relative displacement can be expressed as

$$|\phi_0(t) - \phi_1(t)| = \sqrt{\left[\Re(\phi_{0_0}) - \phi_{1_0}\right]^2 + \left[\Im(\phi_{0_0})\right]^2} \tag{31.25}$$

and then

$$|\phi_0(t) - \phi_1(t)| = \phi_{1_0} \frac{J_s^2\omega^2}{\sqrt{c^2 + J_s^2\omega^2}} \,. \tag{31.26}$$

The energy dissipated in a period by the damper is

$$E_d = \int_0^T c\left[\dot{\phi}_0(t) - \dot{\phi}_1(t)\right]^2 dt = c\phi_{1_0}^2 \pi \frac{J_s^2\omega^4}{c^2 + J_s^2\omega^2}. \tag{31.27}$$

It is easy to verify that both conditions $c = 0$ and $c \to \infty$ lead to a vanishingly small energy dissipation: In the first case because the seismic mass does not interact with the system, and in the second case because nodes 1 and 0 are rigidly connected. The value of the damping coefficient leading to a maximum energy dissipation can be obtained simply by differentiating Eq. (31.27) and equating the derivative to zero

$$J_s^2\omega^2 - c^2 = 0 \,. \tag{31.28}$$

The value of the optimum damping so obtained is

$$c_{opt} = J_s\omega \,. \tag{31.29}$$

Even if the value of the optimum damping depends on the frequency, dampers of the type described here allow a substantial reduction of the amplitude of vibration in a large frequency range.

Because all dissipative dampers convert mechanical energy into heat, they are subject to potentially high temperatures. It is then necessary to verify that they can dissipate all the thermal energy they produce, which can be computed using formulas of the type of Eq. (31.27), at least in terms of average power over a given period of time.

A limit to the ratio between the thermal power and the external surface of the damper is usually assumed. For the type in Fig. 31.5a, for example, it is suggested not to exceed 1.9×10^4 kW/m^2 in continuous operation and 5×10^4 kW/m^2 for short periods of time.

If the seismic mass is connected to the shaft with a torsional spring with non-vanishing stiffness, the device is a true dynamic vibration absorber. Such torsional vibration absorbers introduce a new natural frequency into the system and change the natural frequency on which they are tuned. The distance between the two resonance peaks increases with increasing moment of inertia of the seismic mass. Because an undamped vibration absorber is effective in a very narrow frequency range, outside

of which it is not only ineffective but can cause new resonances, the seismic mass is connected to the shaft through a system that has a certain amount of damping. In such cases it is possible to obtain a response that is fairly flat in an ample range of frequencies.

From a practical viewpoint, all dampers shown in the previous section can be converted into damped vibration absorbers simply by adding an elastic element between the shaft and the seismic mass, which allows the damper to be tuned on the required frequency.

Elastomeric dampers are used on many automotive engines (Fig. 31.5b), particularly on small diesel engines. They may be considered as damped vibration absorbers. The elastomeric elements act as both springs and dampers, and can be designed so as to achieve the required dynamic characteristics. In this case the damper must be designed to take into account the heat generated within the damping element, particularly because the thermal conductivity and mechanical characteristics at high temperature of the rubber are both low. Overheating is particularly dangerous, because any increase of temperature leads to a decrease of the internal damping and then an increase of vibration amplitude. This leads to a further temperature increase until the damper is destroyed, something that could cause severe fatigue problems to the whole system.

31.2.6 Ancillary Equipment

The crankshaft drives a number of ancillary devices that are increasingly common in modern cars. To the camshafts, the generator, the water pump and possibly the fan (which is, however, often driven directly by an electric motor) and other devices such as the power steering pump and the air conditioner compressor must be added. These devices are usually driven through a V or a timing belt, while camshafts are usually driven by a chain or a timing belt. Each shaft has its own speed, so that each transmission has its own transmission ratio. The transmission ratio of the cam shaft is always 1/2.

Ancillary devices may be included in the engine model as well as the driveline by adding other concentrated moments of inertia connected to the main system by secondary shafts that simulate the stiffness of the belt, chain or gearwheel transmission. The same procedure that will be shown when dealing with the driveline may be used to account for the different gear ratios. This approach may, however, be only a first approximation, because the belt usually moves more than one device and is kept tight by tensioners that have their own dynamics based on their mass and stiffness. The belt is then not equivalent to a number of shafts connecting the various devices to the crankshaft. Moreover, the behavior of the belt is often nonlinear.

Because of the presence of many ancillary devices, usually mounted on brackets with a limited stiffness, torsional vibration of the crankshaft causes vibration of the brackets and the masses mounted on them. These vibrations may adversely affect vibrational and acoustic comfort. Because these devices are usually located close to

the cooling air intake, noise caused by their vibration propagates outside the vehicle and contributes to what is usually referred to as acoustic pollution.

Dynamic vibration absorbers or low stiffness joints are often located close to the pulleys driving the belts, to reduce both noise and dynamic stresses. The functions of elastic joint and damper are generally performed by a single device, containing two or more seismic masses, one of which is the outer rim of the pulley driving the belt.

Because the inertia of the ancillary device is not large and the stiffness of the belt or other transmission devices is high, their dynamics lies in a frequency range above that involving the sprung and unsprung mass modes, and primarily affects acoustic comfort.

31.2.7 Engine Control

Variations of the engine torque in time due to the thermodynamic cycle may excite vibrations of the driveline at medium-high frequency. The fundamental harmonic has a frequency $\Omega/2$ in a four-stroke cycle engine, which at 1000 rpm already corresponds to 8 Hz. At the speeds at which the engine usually operates, frequencies are much higher. The other harmonics have a frequency that is a multiple of the fundamental frequency and is often quite high, because 20 or even 25 harmonics must usually be taken into account. At the first natural frequency of the driveline the engine torque can be considered constant in time, as far as the internal dynamics of the engine is concerned. The torque varies according to the commands given by the driver.

In traditional layouts, the engine is controlled by the driver through the accelerator pedal, with commands transmitted to the throttle or injection pump by a mechanical (cable) or hydraulic transmission. Even when the driver manoeuvres the accelerator quite quickly, the command is transferred directly to the engine. The engine torque increases rapidly following a sudden opening or closing of the throttle, with characteristic times typical of those of the thermodynamic cycle: A sort of step input is then occurring, exciting all frequencies up to values of some tens of Hz, or even more. The accelerator manoeuvre may then excite the first torsional frequency of the driveline.

In more modern layouts the transmission of the accelerator control is performed by a *by wire* device: The pedal is connected to a sensor supplying a position signal to the engine control system. In this case it is possible to prevent the transmission natural frequencies from being excited, avoiding high mechanical stresses to the involved elements.

The simplest strategy is to introduce a low-pass filter, cutting out frequencies above a value of about 1 or 2 Hz. This has the advantage of preventing the excitation of the driveline natural frequencies, but the engine becomes less responsive, both when accelerating and slowing down. More complex strategies based on filters that cut out specific frequencies, or provide laws of torque as a function of time to avoid excitation of resonant vibration, require a detailed knowledge of the dynamics of the

driveline and accurate adjustments. Strategies of this type are called open loop or feedforward strategies, because they modify the input of the system (in this case the driving torque) without measuring its effects.

Such an open loop approach may be complemented by measuring the effects of the accelerator manoeuvre, (i.e. acceleration of the vehicle, torsional deformation of the driveline, etc.) and then modifying the command of the throttle or injection pump to limit vibration (closed loop or feedback control).

The model of the driveline must also contain in this case a mathematical model of the device controlling the engine, to simulate specific step input or tip-in, tip-out manoeuvres.

31.2.8 Engine Suspension

The engine suspension system has two primary functions:

- supporting the static and dynamic loads due to the mass of the engine, its reciprocating and rotating elements and driving torque,
- isolating the structure of the vehicle from vibration and noise produced by the propulsion unit, which usually includes the engine, the gearbox and often the differential.

The suspension system should be stiff enough to perform the first task without allowing large displacements and rotations, the limiting case being mounting the engine stiffly on the vehicle body. On the other end, to effectively insulate the vehicle from vibration produced by the propulsion unit, its suspension should be as soft as possible. To strike a compromise between these contrasting requirements, it is of the utmost importance to locate the engine mounts suitably. These are usually elastomeric elements performing the tasks of spring and damper simultaneously.

If the mounts had low stiffness and damping, the engine would behave like a rigid body isolated in space and would transfer no vibration to the structure except that transmitted by the surrounding air. The motion of the engine could then be studied as that of an isolated rigid body on which the actions caused by the pressure of the working gases and the inertia forces caused primarily by imbalance of rotating elements as well as the linear inertia of reciprocating masses are exerted. In this analysis the forcing functions acting on the engine, which are periodic with a period equal to the duration of the thermodynamic cycle (fundamental frequency equal to half the rotation frequency in four-stroke cycle engines), may be developed in Fourier series. The static (zero-frequency) component due to weight and the constant component of the driving torque must be neglected in this computation, because it would lead to a non-periodic motion of the engine that is not supported in any way.

If the motion of the engine as an insulated rigid body under the action of dynamic forces were such that we could identify points where the amplitude vanishes, locating the supports in those points would allow the engine to be supported without transmitting dynamic loads. In actual conditions this is not possible, but analysis of

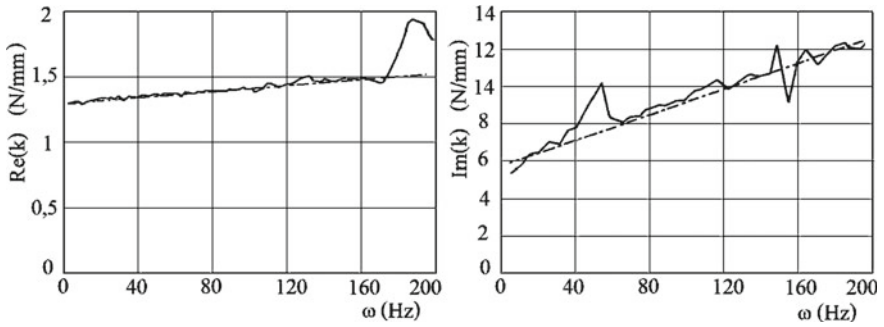

Fig. 31.6 Real (in-phase) and imaginary (in quadrature) parts of the complex stiffness of a support for engine suspension versus the frequency

the free motion allows us to identify points where the amplitude of that motion is relatively small. We can then identify configurations from which the optimization of the engine suspension geometry can begin, taking into account the compliance of the structure supporting the engine.

Among the possible layouts for engine suspensions, those based on three supports, and on two supports withstanding the weight of the engine plus a link, itself attached through elastomeric supports, to withstand the engine torque, must be mentioned. The latter solution allows a high rotational stiffness to be obtained, accompanied by a moderate translational stiffness.

The concept of complex stiffness may be used to identify an in-phase and an in-quadrature stiffness, both functions of frequency, and then to describe the elastic and damping behavior of the supports under a harmonic forcing function. The characteristics of one of the supports of an engine suspension are shown in Fig. 31.6 as an example. Supports with controllable characteristics and active supports have been built and applied on some vehicles.

Remark 31.7 Engine suspension may have a strong influence not only on insulation from vibration and noise produced by the engine, but also on riding comfort, because the engine is quite a large mass suspended through an elastic and damping system that couples it to the heave and pitch dynamics of the vehicle and also, even if to a lesser extent, to the torsional dynamics of the driveline.

31.3 Driveline

The driveline, including shafts, gear wheels, joints and other elements such as the clutch with related damper springs, may be modelled as a lumped parameters system (made by massless shafts where the elastic properties of the system are concentrated) with lumped masses modelling its inertial properties.

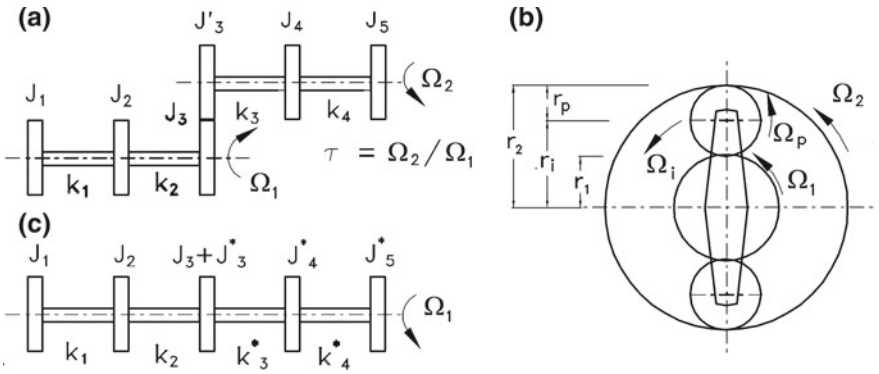

Fig. 31.7 Geared system: Sketch of the **a** actual system and **b** equivalent system; **c** planetary gear train. Sketch of the system and notation

The damping of the system may be neglected altogether, or modelled by introducing suitable viscous dampers in parallel to the springs modelling the various parts of the shaft and joints.

If the clutch is assumed to be fully engaged and the gearbox is in a given gear, the configuration of the driveline is fixed. There is then no difficulty in building a simple mathematical model of the entire system.

Nor does the fact that the various elements of the driveline rotate at different speeds cause problems. Consider the system sketched in Fig. 31.7a, in which the two shafts are linked by a pair of gear wheels, with transmission ratio τ. For the study of the torsional vibrations of the system, it is possible to replace the system with a suitable equivalent, in which one of the two shafts is replaced by an expansion of the other (Fig. 31.7b).

Assuming as well that the deformation of gear wheels is negligible, the equivalent rotations ϕ_i^* may be obtained from the actual rotations ϕ_i simply by dividing the latter by the transmission ratio $\tau = \Omega_2/\Omega_1$,

$$\phi_i^* = \frac{\phi_i}{\tau}. \tag{31.30}$$

The kinetic energy of the ith flywheel, whose moment of inertia is J_i, and the elastic potential energy of the ith span of the shaft are, respectively,

$$\begin{aligned} \mathcal{T} &= \tfrac{1}{2} J_i \dot{\phi}_i^2 = \tfrac{1}{2} J_i^* \dot{\phi}_i^{*^2}, \\ \mathcal{U} &= \tfrac{1}{2} k_i \left(\phi_{i+1}^2 - \phi_i^2\right) = \tfrac{1}{2} k_i^* \left(\phi_{i+1}^{*^2} - \phi_i^{*^2}\right), \end{aligned} \tag{31.31}$$

where the equivalent moment of inertia and stiffness are, respectively,

$$J_i^* = \tau^2 J_i, k_i^* = \tau^2 k_i \,. \tag{31.32}$$

The moments of inertia and the torsional stiffness of the various elements of the geared system can thus be reduced to the main system simply by multiplying them by the square of the gear ratio

$$c_i^* = \tau^2 c_i \ . \tag{31.33}$$

In the same way, if damping of the shafts is accounted for by introducing dampers in parallel to the springs, the damping coefficient must be multiplied by the square of the gear ratio.

If the system includes a planetary gear train, the computation can be performed without difficulties. The equivalent stiffness can be computed simply from the overall transmission ratio. The total kinetic energy of the rotating parts must be taken into account when computing the equivalent inertia. The angular velocities of the central gear Ω_1, of the ring gear Ω_2, of the revolving carrier Ω_i, and of the intermediate pinions Ω_p of the planetary gear shown in Fig. 31.7c are linked by the equation

$$\frac{\Omega_1 - \Omega_i}{\Omega_2 - \Omega_i} = -\frac{r_2}{r_1} \quad , \quad \Omega_p = (\Omega_1 - \Omega_i)\frac{r_1}{r_p} - \Omega_i . \tag{31.34}$$

The equivalent moment of inertia of the system made of the internal gear, with moment of inertia J_1, the ring gear, with moment of inertia J_2, the revolving carrier, with moment of inertia J_i, and n intermediate pinions, each with mass m_p and moment of inertia J_p, referred to the shaft of the internal gear is

$$J_{eq} = J_1 + J_2 \left(\frac{\Omega_2}{\Omega_1}\right)^2 + (J_i + n m_p r_i^2)\left(\frac{\Omega_i}{\Omega_1}\right)^2 + n J_p \left(\frac{\Omega_p}{\Omega_1}\right)^2 . \tag{31.35}$$

If the deformation of the meshing teeth must be accounted for, it is possible to introduce two separate degrees of freedom for the two meshing gear wheels into the model, modeled as two different inertias, and to introduce a shaft between them whose compliance simulates the compliance of the transmission. This is particularly important when a belt or flexible transmission of some kind is used instead of the stiffer gear wheels. In a driveline there may be several shafts connected to each other, in series or in parallel, by gear wheels with different transmission ratios.

The equivalent system is referred to one of the shafts and the equivalent inertias and stiffness of the elements of the others are all computed using the ratios between the speeds of the relevant element and the reference shaft. The equivalent system will then be made of a set of elements, in series or in parallel, following the scheme of the actual system, but with rotations that are all consistent.

If the compliance of the gears is to be accounted for in detail, the nonlinearities due to the contacts between the meshing teeth and backlash must be considered, as will be seen later.

The driveline may cause comfort problems not only in terms of its torsional compliance, but also its bending compliance. The propeller shaft and the wheel

shafts have their own flexural natural frequencies and critical speeds. They may cause severe vibration when they operate close to a critical speed.

Without entering into details about the dynamic behavior of rotating elements,[3] the following considerations can be advanced.

- The gyroscopic effects of transmission shafts are weak. Critical speeds are close to the natural frequencies when the system is not rotating.
- The balance conditions of the rotating elements have no effect on the natural frequency or the critical speed, but do determine the strength of the excitation at such speeds.
- The damping of the shaft (and the joints) has no effect in limiting the amplitude of vibration at the critical speeds, while the damping of the supports (non-rotating damping) is essential to this aim.

The critical speeds of the wheel shafts are generally beyond the working range and thus do not cause resonant vibration. However, the first critical speed of the propeller shaft in vehicles with front engine and rear wheel drive is in the working range. The critical speed of traditional propeller shafts, in two parts with a Hooke joint and elastic support in the middle, occurs when the vehicle travels at a low speed: The shaft then works normally in the supercritical regime, when self-centred.

The shaft and above all the joint must be accurately balanced, so as to go through the critical speed without strong vibration, while the central support must supply enough damping. The damping of the support is also needed to prevent the crossing of an instability threshold in high speed operation.

Cars with front engine and rear wheel drive are prone to vibrate strongly when passing through the critical speed of the propeller shaft if the balancing of the central joint deteriorates or the elastic and above all damping properties of the support become worse due to aging or wear.

Misalignment of the propeller shaft or wheel shafts may also cause the driveline to vibrate.

31.4 Inertia of the Vehicle

The tires may be considered as rigid bodies, allowing longitudinal slip to be neglected when performing a first approximation study. In this case the vehicle inertia and the resistance to motion may be accounted for as seen in Chap. 23 in the study of the take-off manoeuvre. The vehicle may then be modelled as a flywheel, connected after the wheel shafts that, in the equivalent system, rotate at the same speed as the engine.

Taking into account the inertia of all wheels, the moment of inertia of this flywheel is

[3] See, for instance, G. Genta, *Dynamics of rotating systems*, Springer, New York, 2005.

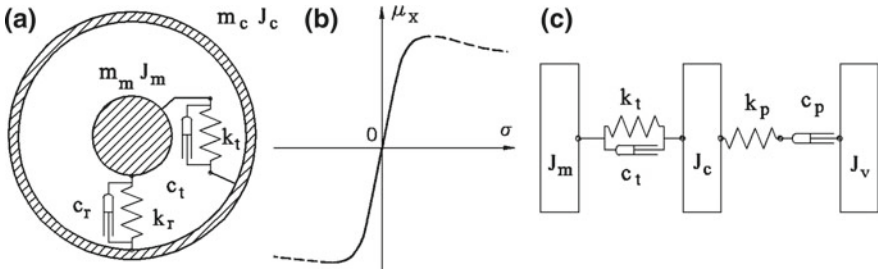

Fig. 31.8 Model of the tire and the tire-road contact. **a** Dynamic model of the tire; **b** Force-longitudinal slip characteristic for the tire. **c** Dynamic model of the tire-road contact (the moments of inertia and the torsional characteristics are drawn as masses and translational characteristics)

$$J_v = \left(m + \sum_{\forall i} \frac{J_{ri}}{R_{ei}^2} \right) R_e^2 \tau^2 \ , \tag{31.36}$$

where J_{ri} is the moment of inertia of the ith wheel, which may have different equivalent rolling radii, R_e is the equivalent rolling radius of the driving wheels and τ is the overall gear ratio between engine and wheels.

The drag torque M_r applied to the flywheel simulating the vehicle is

$$M_r = F_r R_e \tau \ , \tag{31.37}$$

where the total resistance to motion (road load) F_r depends on the speed following Eq. (23.17):

$$F_r = A + BV^2 + CV^4 \ ,$$

and the expressions for constants A, B and C[4] are as reported in Chap. 23.

For a more detailed study, both the compliance of the tire and its longitudinal slip at the wheel-road contact must be accounted for. The simplest way to model the former is by simulating the tire as a rigid ring, with mass m_c and moment of inertia J_c, corresponding to the tread band and the belt beneath it. This is connected to the wheel hub, whose mass and moment of inertia are m_m and J_m through an elastic system having a radial and torsional stiffness equal to k_r and k_t respectively.

The rim and hub are also assumed to be rigid bodies. Viscous dampers with coefficients c_r and c_t (Fig. 31.8a) may be added in parallel to the springs. The masses and the radial stiffness and damping are included in the ride comfort models, as seen in the previous chapter, while the moments of inertia and the torsional stiffness and damping are included in the driveline and longitudinal models.

The wheel-ground contact may be characterized by the plot of the longitudinal force coefficient versus the sideslip $\mu_x(\sigma)$ (Fig. 31.8b). Usually only the first part

[4]Parameters A, B and C used in the equation giving the road load must not be confused with the parameters with the same name included in the magic formula.

of the curve, approximated as a straight line, is used in the study of the driveline dynamics. The slope of the line may be easily obtained from the coefficients of the magic formula and is given by product BCD.

The longitudinal slip σ is linked to the ratio between the speed Ω_c of the wheel and the speed of the moment of inertia simulating the vehicle

$$\Omega_v = \frac{V}{R_e}$$

by the relationship

$$\sigma = \frac{\Omega_c}{\Omega_v} - 1 \, .$$

The longitudinal force the tire exerts is then

$$F_x = F_z \mu_x = b F_z \sigma = b F_z \left(\frac{\Omega_c - \Omega_v}{\Omega_v} \right) \, , \tag{31.38}$$

where

$$b = BCD \, .$$

The moment exerted on the wheel due to the longitudinal slip is

$$M = R_e F_x = \frac{b F_z R_e}{\Omega_v} \left(\Omega_c - \Omega_v \right) \, . \tag{31.39}$$

The wheel-ground contact may then be modelled as a viscous damper with damping coefficient

$$c_p = \frac{b F_z R_e^2}{V} \, . \tag{31.40}$$

Coefficient c_p depends first upon the vehicle speed and then upon the variable of motion Ω_v: the equation of motion is then nonlinear. For small velocity variations it is, however, possible to linearize the equations by using an average value of the speed in the expression of c_p. When the speed tends to zero, the damping coefficient tends to infinity: This linearized model cannot be used in the first instants of a take-off manoeuvre, when the vehicle is still stationary, because in these conditions the longitudinal slip is high, or better tends to infinity.

The tire model is usually complemented by adding a spring in series with the damper. Its stiffness is

$$k_p = \frac{b F_z R_e^2}{a} \, , \tag{31.41}$$

where a is a length equal to half the length of the contact zone.

Stiffness k_p can be suitably modified to take into account the longitudinal compliance of the suspension of the driving wheels.

The tire is then modelled with two moments of inertia connected to each other with a spring and a damper in parallel, and connected to the flywheel simulating the vehicle with a spring and a damper in series. The model is sketched in Fig. 31.8c, where the torsional springs and the moments of inertia are drawn as springs and masses.

31.5 Linearized Driveline Model

A driveline model from the engine to the vehicle can thus be assembled using the partial models seen above. As already stated, the elements to be taken into account depend upon the aim for which the model has been built. A relatively simple model is shown in Fig. 31.9a. If low frequency oscillations, such as those occurring in tip-in, tip-out manoeuvres, are to be studied, the engine can be modelled as a single moment of inertia. The two wheel shafts are modelled separately in this model, because in many cars with transversal front engine and front-wheel drive their stiffnesses are different. However, the two branches of the driveline can be joined if a first approximation study of the low frequency dynamics alone is required (Fig. 31.9b). This can be done by introducing inertias and stiffnesses equal to the sum of those of the single branches.

The model shown in Fig. 31.9a has 10 degrees of freedom. Because two of them have a vanishing associated mass, it has only 18 state variables. The generalized coordinates are the rotations of the various moments of inertia. It is possible to order

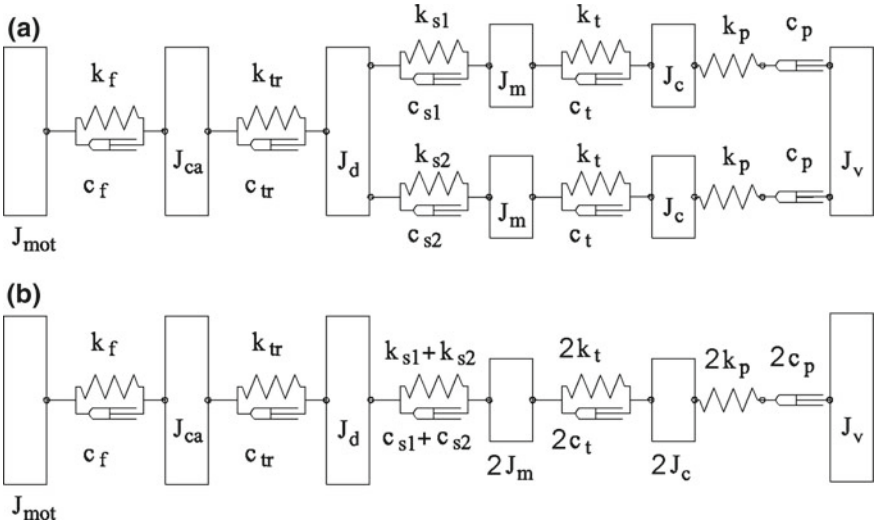

Fig. 31.9 Model of the driveline for the study of low frequency dynamics (**a**), and model in which the presence of two separate wheel shafts is neglected (**b**)

them by separating the nodes where there is a mass from those that are massless. Thus

$$\mathbf{x} = \left[\mathbf{x}_1^T \ \mathbf{x}_2^T \right]^T \ , \tag{31.42}$$

where

$$\mathbf{x}_1 = \left[\theta_{mot} \ \theta_{ca} \ \theta_d \ \theta_{m1} \ \theta_{m2} \ \theta_{c1} \ \theta_{c2} \ \theta_v \right]^T \ ,$$

$$\mathbf{x}_2 = \left[\theta_{i1} \ \theta_{i2} \right]^T \ .$$

The mass matrix of the system may be partitioned in four parts as

$$\mathbf{M} = \begin{bmatrix} \mathbf{M}_{11} \ \mathbf{M}_{12} \\ \mathbf{M}_{21} \ \mathbf{M}_{22} \end{bmatrix} \tag{31.43}$$

where

$$\mathbf{M}_{11} = \text{diag} \left[J_{mot} \ J_{ca}^* \ J_d^* \ J_m^* \ J_m^* \ J_c^* \ J_c^* \ J_v^* \right] \tag{31.44}$$

and all other sub-matrices are null.

The stiffness matrix may be partitioned in the same way

$$\mathbf{K}_{11} = \begin{bmatrix} k_f & -k_f & 0 & 0 & 0 & 0 & 0 & 0 \\ & k_f + k_{tr}^* & -k_{tr}^* & 0 & 0 & 0 & 0 & 0 \\ & & k_1 & -k_{s1}^* & -k_{s2}^* & 0 & 0 & 0 \\ & & & k_{s1}^* + k_t^* & 0 & -k_t^* & 0 & 0 \\ & & & & k_{s2}^* + k_t^* & 0 & -k_t^* & 0 \\ & & & & & k_t^* + k_p^* & 0 & 0 \\ & & & & & & k_t^* + k_p^* & 0 \\ & \text{symm.} & & & & & & 0 \end{bmatrix} , \tag{31.45}$$

where

$$k_1 = k_{tr}^* + k_{s1}^* + k_{s2}^* \ ,$$

$$\mathbf{K}_{21} = \left[\mathbf{0}_{2\times 5} \begin{bmatrix} -k_p^* & 0 & 0 \\ 0 & -k_p^* & 0 \end{bmatrix} \right] , \tag{31.46}$$

$$\mathbf{K}_{22} = \begin{bmatrix} k_p^* & 0 \\ 0 & k_p^* \end{bmatrix} , \quad \mathbf{K}_{12} = \mathbf{K}_{21}^T . \tag{31.47}$$

In a similar way the submatrices of the damping matrix are

$$\mathbf{C}_{11} = \begin{bmatrix} c_f & -c_f & 0 & 0 & 0 & 0 & 0 & 0 \\ & c_f + c_{tr}^* & -c_{tr}^* & 0 & 0 & 0 & 0 & 0 \\ & & c_1 & -c_{s1}^* & -c_{s2}^* & 0 & 0 & 0 \\ & & & c_{s1}^* + c_t^* & 0 & -c_t^* & 0 & 0 \\ & & & & c_{s2}^* + c_t^* & 0 & -c_t^* & 0 \\ & & & & & c_t^* & 0 & 0 \\ & & & & & & c_t^* & 0 \\ & \text{symm.} & & & & & & 2c_p^* \end{bmatrix} , \tag{31.48}$$

where

$$c_1 = c_{tr}^* + c_{s1}^* + c_{s2}^* ,$$

$$\mathbf{C}_{21} = \begin{bmatrix} \mathbf{0}_{2\times 7} \begin{bmatrix} -c_p^* \\ -c_p^* \end{bmatrix} \end{bmatrix} , \mathbf{C}_{22} = \begin{bmatrix} c_p^* & 0 \\ 0 & c_p^* \end{bmatrix} , \mathbf{C}_{12} = \mathbf{C}_{21}^T . \tag{31.49}$$

The assumption that the damping of the various components of the driveline can be modelled as viscous is only approximate, but it cannot be modelled as hysteretic damping (which is not much better for elements like the clutch damper springs) because that would not allow the numerical simulation of manoeuvres such as the response to a step input. However, because the phenomenon here studied occurs at a well determined frequency, it is possible to approximate hysteretic damping with an equivalent viscous damping

$$c_{eq} = \frac{\eta k}{\omega} , \tag{31.50}$$

where η and k are the loss factor and the stiffness of the relevant elements and ω is the frequency of the oscillations of the driveline. It is possible to perform a first computation with no damping (except that used to simulate tire slip) to compute a value for the frequency of the free oscillations, and then to proceed with calculations that include an equivalent damping.

The state vector can be written in the form

$$\mathbf{z} = \begin{bmatrix} \mathbf{v}_1^T & \mathbf{x}_1^T & \mathbf{x}_2^T \end{bmatrix}^T , \tag{31.51}$$

where $\mathbf{v}_1$ contains the derivatives of coordinates $\mathbf{x}_1$.

The state equation is then

$$\begin{bmatrix} \mathbf{M}_{11} & \mathbf{0} & \mathbf{C}_{12} \\ \mathbf{0} & \mathbf{0} & \mathbf{C}_{22} \\ \mathbf{0} & \mathbf{I} & \mathbf{0} \end{bmatrix} \dot{\mathbf{z}} = - \begin{bmatrix} \mathbf{C}_{11} & \mathbf{K}_{11} & \mathbf{K}_{12} \\ \mathbf{C}_{21} & \mathbf{K}_{21} & \mathbf{K}_{22} \\ -\mathbf{I} & \mathbf{0} & \mathbf{0} \end{bmatrix} \mathbf{z} + \begin{Bmatrix} \mathbf{F}_1 \\ \mathbf{0} \\ \mathbf{0} \end{Bmatrix} , \tag{31.52}$$

where vector $\mathbf{F}_1$ contains the moments applied on the nodes whose coordinates are included in vector $\mathbf{x}_1$. Because only the driving and drag torques are present, it follows that

$$\mathbf{F}_1 = \begin{Bmatrix} M_{mot} \\ \mathbf{0}_{6\times 1} \\ M_r \end{Bmatrix} . \tag{31.53}$$

The dynamic matrix of the system is then

$$\mathbf{A} = -\begin{bmatrix} \mathbf{M}_{11} & \mathbf{0} & \mathbf{C}_{12} \\ \mathbf{0} & \mathbf{0} & \mathbf{C}_{22} \\ \mathbf{0} & \mathbf{I} & \mathbf{0} \end{bmatrix}^{-1} \begin{bmatrix} \mathbf{C}_{11} & \mathbf{K}_{11} & \mathbf{K}_{12} \\ \mathbf{C}_{21} & \mathbf{K}_{21} & \mathbf{K}_{22} \\ -\mathbf{I} & \mathbf{0} & \mathbf{0} \end{bmatrix} . \tag{31.54}$$

Example 31.1 Simulate a tip-in, tip-out manoeuvre in second gear with engine at 1,500 rpm. With the vehicle running at constant speed (driving torque equal to drag torque) increase suddenly the driving torque to its maximum value and keep such a value until 2,000 rpm. are reached. The accelerator is then fully released and the vehicle slows down.

Data: maximum driving torque: $M_{\max} = 40$ Nm; braking torque of the engine: $M_f = -4$ Nm.

Vehicle: Mass $m = 950$ kg, $f_0 = 0.013$, $K = 6.5 \times 10^{-6}$ s^2/m^2, $C_x = 0.32$, $S = 1.7$ m^2, $R_e = 257$ mm, half-length of the contact area $a = 50$ mm. Neglect the efficiency of the transmission.

Moments of inertia: Engine (including the flywheel) $J_{mot} = 0.125$ kg m^2, gear $J_{ca} = 0.0045$ kg m^2, differential $J_d = 0.065$ kg m^2, wheel hub $J_m = 0.3$ kg m^2, thread band $J_c = 0.32$ kg m^2.

Stiffnesses: Clutch disk (with damper springs, when driving), $k_f = 975$ Nm/rad, wheel shafts $k_{s1} = 7{,}500$ Nm/rad, $k_{s2} = 10{,}400$ Nm/rad, tire $k_t = 59{,}000$ Nm/rad.

Neglect the damping of the driveline elements.

Gear ratios: Final gear $\tau_p = 0.2884$; gearbox (second gear) $\tau_c = 23/63$.

By using the tire model previously used to compute the contact parameters, stiffness b is

$$b = A\left(\frac{K}{\alpha + d}\right)^{1/n} - D ,$$

where $\alpha = 0$ (there is no sideslip angle), $A = 1.12$, $K = 46$, $n = 0.6$, $d = 5$, $D = 1$.

The compliance of the gearbox-differential connection is neglected and then a single moment of inertia $J_{ca} = 0.0695$ kg m^2 is assumed for gearbox and differential, located on the gearbox output shaft.

The values of the inertias and stiffnesses, reduced to the engine shaft (multiplied by the squares of the transmission ratios) are: $J^*_{ca} = 0.00926$ kg m^2, $J^*_m = 0.00333$ kg m^2, $J^*_c = 0.00355$ kg m^2, $k^*_{s1} = 83.14$ Nm/rad, $k^*_{s2} = 115.3$ Nm/rad, $k^*_t = 654.1$ Nm/rad.

The moment of inertia of the vehicle reduced to the engine shaft, including also the two free wheels as well, is $J^*_v = 0.696$ kg m^2.

The speed of the vehicle at 1,500 rpm is $V = 4.25$ m/s $= 15.30$ km/h.

Neglecting the term of the road load in V^4, the drag moment reduced to the engine shaft may be written as

$$M_r = R R_e \tau^2 = A_r + B_r \Omega_v^2 ,$$

where $A_r = 3.28$ Nm, $B_r = 8.15 \times 10^{-6}$ Nms^2. The drag torque at 1,500 rpm is 3.48 Nm: Predictably, the quadratic term as a small effect at such a low speed.

Coefficients c_p and k_p are $c_p = 1{,}913$ Nms/rad and $k_p = 163{,}000$ Nm/rad at a speed of 1,500 rpm. It then follows that $c_p^* = 21.21$ Nms/rad and $k_p^* = 1{,}803$ Nm/rad.

Natural frequencies are immediately obtained from the eigenvalues of the dynamic matrix. Three eigenvalues are equal to zero, because rigid body modes are possible. The eigenvalue with the smallest imaginary part, i.e. that corresponding to motion with the lowest natural frequency, is

$$s = -1.69 \pm 35.58\, i \ \text{1/s} ,$$

and the corresponding frequency of the damped free oscillations is 5.66 Hz. It is the low frequency mode typical of the phenomenon under study.

The following eigenvalue is

$$s = -4.32 \pm 347\, i \ \text{1/s} ,$$

corresponding to a damped oscillation with a frequency of 55.23 Hz. This is almost ten times the frequency of the lowest mode. To study oscillations at this frequency it is advisable to use a more detailed model.

The results of the tip-in, tip-out manoeuvre are shown in Fig. 31.10. In (a) the time histories of the velocity of engine and vehicle are reported, while the longitudinal acceleration of the vehicle is plotted in (b). By comparing the results of the simulation with those shown in Fig. 31.1, a qualitative similarity is found, although the results refer to different vehicles. The longitudinal acceleration computed in the simulation is that of the wheel hub, while the experimental results were measured in the passenger compartment and then filtered by the structure of the vehicle. Moreover, the mathematical model does not take into account the damping of the driveline, but only that caused by tire slip.

Example 31.2 Repeat the simulation of the previous example, taking into account n hysteretic damping with a loss factor $\eta = 0.2$ for the clutch damper springs and $\eta = 0.05$ for all other elements. To convert hysteretic into viscous damping, the equivalent damping at a frequency of 35.58 rad/s is computed.

The eigenvalue with the lowest imaginary part, i.e. that corresponding to the oscillations with the lowest frequency, is now

$$s = -2.88 \pm 35.43\, i \ \text{1/s} ,$$

corresponding to oscillations at a frequency of 5.64 Hz. By comparing this result with that seen above, it is clear that the decay rate has increased considerably (it almost doubled), while the frequency is essentially the same.

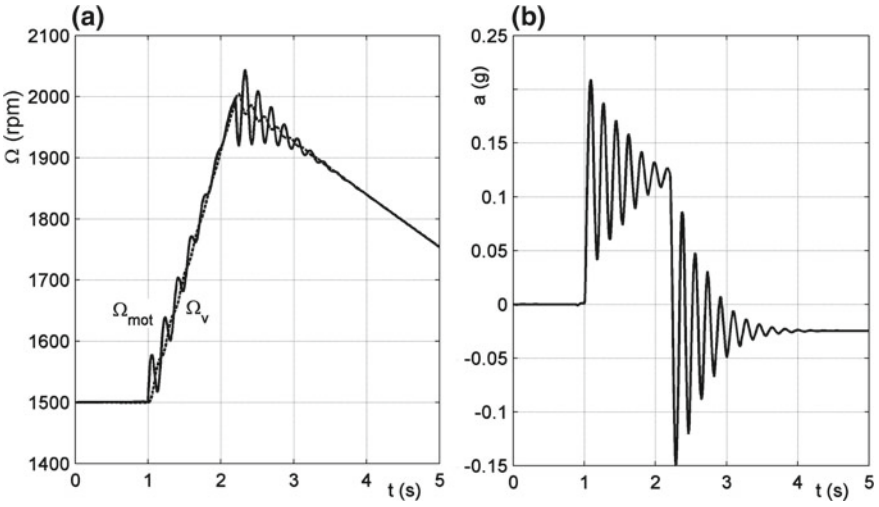

Fig. 31.10 Results of a tip-in, tip-out manoeuvre. **a** Engine and wheel speeds (reduced to the engine shaft); **b** longitudinal acceleration of the vehicle

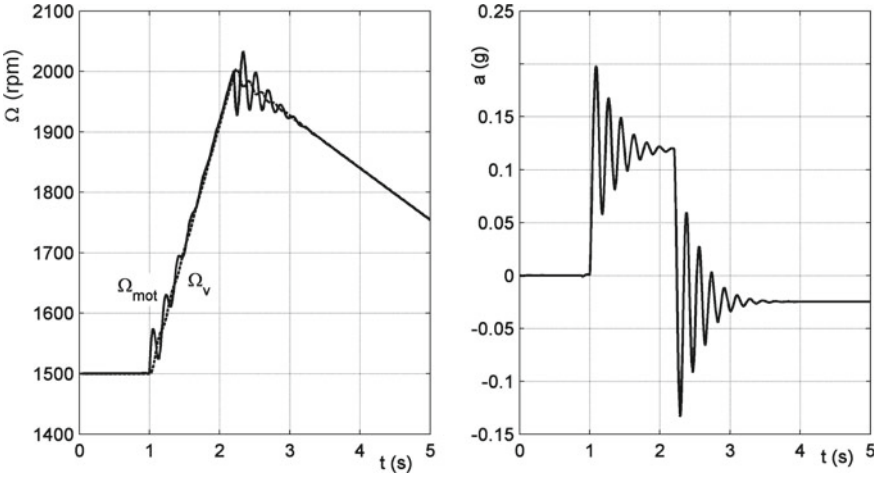

Fig. 31.11 Results of a tip-in, tip-out manoeuvre, computed while taking into account the damping of the various elements. **a** Engine and wheel speeds (reduced to the engine shaft); **b** longitudinal acceleration of the vehicle

The results of the simulation are reported in Fig. 31.11. The effect of damping is fairly limited: the oscillations damp out in a shorter time, but the maximum values of the acceleration are little changed.

31.6 Non-time-Invariant Models

If the torsional vibration of the driveline must be studied with the reciprocating masses in the engine in mind, a model with inertial properties that are variable in time must be used.

Three different approaches are possible. Listing them in order of increasing complexity, they are

1. Traditional approach. The effect of the variable component of the moments of inertia of the crank systems is modelled as a torque with known time history applied to the node where the crank is located. Because the model is linearized, it is possible to write the frequency domain equations and to solve them analytically.
2. Approach in which the torsional deformations are considered small and the corresponding angles can be neglected in the computation of the inertia of the cranks. The equations of motion, nonlinear and non-time-invariant, have coefficients with a known time history. No closed form of the equations of motion is possible, and numerical integration is needed.
3. Approach with no particular simplifying assumption. The equations of motion must be solved numerically, but the solution is much more difficult than in case (2).

31.6.1 Equations of Motion

The equation of motion of the engine-driveline system can be obtained in the usual way, using Lagrange equations. The system may be modelled starting from a lumped parameters approach, obtaining a model of the type shown in Fig. 31.9a, with the difference that now the engine is not lumped in a single inertia, but is modelled as another lumped parameter system, with the various moments of inertia modelling cranks, flywheel, ancillary devices, dampers, etc. connected to each other by torsional springs and dampers. The system may be in-line, like that in Fig. 31.9b, or multiply connected, like that in Fig. 31.9a.

There is no difficulty in linearizing the elastic and dissipative part of the system by writing stiffness and damping matrices $\mathbf{K}$ and $\mathbf{C}$. The stiffnesses of the part modelling the engine will be the equivalent stiffnesses and the damping coefficients of the same elements can be computed as seen above. The potential energy and the dissipation functions will have the structure typical of linear systems

$$\mathcal{U} = \frac{1}{2}\mathbf{x}^T\mathbf{K}\mathbf{x}, \mathcal{F} = \frac{1}{2}\dot{\mathbf{x}}^T\mathbf{C}\dot{\mathbf{x}} \,. \tag{31.55}$$

The mass matrix can be computed using the methods seen for the equivalent system

$$\mathbf{M} = \text{diag}\left[J_{eq_i}\right] \,, \tag{31.56}$$

but here the equivalent moments of inertia of the cranks are functions of their rotation angles and then of their generalized coordinates. The mass matrix is still diagonal, so that the element at the ith row and ith column depends only upon the ith generalized coordinate. Because the equivalent moment of inertia must be written as a Fourier series (Eq. 31.12), it follows that

$$\mathbf{M} = \mathbf{M}_0 + \mathbf{M}_1 (\mathbf{x}) = \text{diag}\,[J_{0i}] + \text{diag}\,[J_{1i} (\theta_i)] \ , \tag{31.57}$$

where:

- $\mathbf{M}_0$ is a diagonal matrix containing the average values of the moments of inertia of the cranks and the moments of inertia at all other nodes. Except for the nodes with which no inertia is associated, the elements are all non-zero and their values are J_{0i}.
- $$J_{1i} (\theta_i) = \sum_{k=1}^{m} [J_{cik} \cos(k\theta_i + \delta_{ik}) + J_{sik} \sin(k\theta_i + \delta_{ik})] ; \tag{31.58}$$

  where i is the subscript referring to the node ($i = 1, ..., n$);
- k is the subscript referring to the relevant harmonics and thus spans from 1 to m, the number of the harmonics considered in the series (in theory $m = \infty$);
- θ_i is the rotation angle of the ith node, and thus is the ith element of vector $\mathbf{x}$;
- J_{cik} and J_{sik} are the coefficients of the terms in sine and cosine of the Fourier series for the equivalent moments of inertia. These vanish for all the nodes where no crank is located and are equal for all cranks (they do not depend on subscript i) if the crank systems are all equal;
- δ_{ik} are the phases of the various harmonics in the various cranks, as given by the phase angle diagrams.

The kinetic energy is then

$$\mathcal{T} = \frac{1}{2} \dot{\mathbf{x}}^T \mathbf{M} \dot{\mathbf{x}} \ . \tag{31.59}$$

Assuming that the rotation angle θ_i of the ith node is given by the sum of an average angle θ_0 of the driveline and a torsion angle ϕ_i :

$$x_i = \theta_0 + \phi_i \ , \tag{31.60}$$

for the first $n - 1$ nodes and

$$x_n = \theta_{0v} + \phi_n \ , \tag{31.61}$$

for the last node where the moment of inertia simulating the vehicle is located.

Remark 31.8 The latter node must be kept separate, because, owing to the longitudinal slip of the tire, the average rotations of the driveline and the vehicle θ_0 and θ_{0v} diverge in time.

Let $\mathbf{S}$ be a vector of order $n-1$, whose components are all equal to 1. It is then possible to write

$$\mathbf{x} = \left\{ \begin{matrix} \theta_0 \mathbf{S} \\ \theta_{0v} \end{matrix} \right\} + \phi \, . \tag{31.62}$$

Remembering that the last row and the last column of matrix $\mathbf{K}$ vanish (Eq. (31.45), where all nodes are present), the potential energy is

$$\mathcal{U} = \frac{1}{2}\theta_0^2 \mathbf{S}^T \mathbf{K}^* \mathbf{S} + \frac{1}{2}\phi^{*T} \mathbf{K}^* \phi^* + \theta_0 \mathbf{S}^T \mathbf{K}^* \phi^* \, , \tag{31.63}$$

where $\mathbf{K}^*$ and ϕ^* are the stiffness matrix and the vector of the generalized coordinates without the the last row and column and without the last row respectively.

Rotation expressed by vector $\theta_0 \mathbf{S}$ is a rigid rotation. Because the driveline is free to rotate, product $\mathbf{K}^* \mathbf{S}$ is null and thus it follows that

$$\mathcal{U} = \frac{1}{2}\phi^{*T} \mathbf{K}^* \phi^*, \tag{31.64}$$

i.e.

$$\mathcal{U} = \frac{1}{2}\phi^T \mathbf{K} \phi. \tag{31.65}$$

In a similar way,

$$\dot{\mathbf{x}} = \left\{ \begin{matrix} \Omega_t \mathbf{S} \\ \Omega_v \end{matrix} \right\} + \dot{\phi} \, , \tag{31.66}$$

where Ω_t and Ω_v are the average velocities of the driveline and the vehicle.

The damping matrix may be subdivided into three parts

$$\mathbf{C} = \mathbf{C}_1 + \mathbf{C}_2 + \mathbf{C}_3 \tag{31.67}$$

where

- $\mathbf{C}_1$ is a diagonal matrix, where all dampings toward the ground are listed, that is, all terms expressed by Eq. (31.21) to simulate the energy losses due to the absolute rotation of the nodes,
- $\mathbf{C}_2$ is a matrix with the structure shown in Eq. (31.48) where all nodes are present and the damping c_p simulating the tire slip is not included,
- $\mathbf{C}_3$ is a matrix of type shown in Eq. (31.48) where all nodes are present; it contains only the damping c_p simulating the tire slip.

The dissipation function is then

$$\mathcal{F} = \frac{1}{2} \left(\left\{ \begin{matrix} \Omega_t \mathbf{S} \\ \Omega_v \end{matrix} \right\} + \dot{\phi} \right)^T (\mathbf{C}_1 + \mathbf{C}_2 + \mathbf{C}_3) \left(\left\{ \begin{matrix} \Omega_t \mathbf{S} \\ \Omega_v \end{matrix} \right\} + \dot{\phi} \right) \, , \tag{31.68}$$

that is, performing the products and remembering the properties of the involved matrices

$$\mathcal{F} = \frac{1}{2} \left\{ \begin{array}{c} \Omega_t \\ \Omega_v \end{array} \right\} \left[\begin{array}{cc} \sum_{i=1}^{n-1} c_{1i} + 2c_p & -2c_p \\ -2c_p & 2c_p \end{array} \right] \left\{ \begin{array}{c} \Omega_t \\ \Omega_v \end{array} \right\} + \\ + \left\{ \begin{array}{c} \Omega_t \mathbf{S} \\ \Omega_v \end{array} \right\}^T (\mathbf{C}_1 + \mathbf{C}_3) \dot{\boldsymbol{\phi}} + \frac{1}{2} \dot{\boldsymbol{\phi}}^T \mathbf{C} \dot{\boldsymbol{\phi}} \,. \tag{31.69}$$

In a similar way, remembering that the mass matrix is diagonal, it is possible to write

$$\mathcal{T} = \frac{1}{2} \sum_{i=1}^{n-1} \left[J_{0i} + J_{1i} \left(\theta_i \right) \right] \left(\Omega_t + \dot{\phi}_i \right)^2 + \frac{1}{2} J_{0n} \left(\Omega_v + \dot{\phi}_n \right)^2 \,. \tag{31.70}$$

31.6.2 Rigid-Body Motion of the Driveline

The generalized coordinates are the average rotations of the driveline and the flywheel simulating the vehicle (or better, their derivatives Ω_t and Ω_v) and the torsional rotations ϕ_i of the various elements. It is possible to assume that the low frequency dynamics (actually a non-periodic dynamics) may be studied separately from the torsional dynamics of the system.

When studying the first, the equations simplify: Not only the terms containing $\boldsymbol{\phi}$ vanish, but if the cranks are all equal and (angularly) uniformly spaced, it follows that

$$\sum_{i=1}^{n-1} J_{1i} \left(\theta_i \right) = 0 \quad , J_{tot} = \sum_{i=1}^{n-1} J_{0i} \,. \tag{31.71}$$

Neglecting torsional rotations, it follows that

$$\mathcal{U} = 0, \tag{31.72}$$

$$\mathcal{F} = \frac{1}{2} \left\{ \begin{array}{c} \Omega_t \\ \Omega_v \end{array} \right\} \left[\begin{array}{cc} \sum_{i=1}^{n-1} c_{1i} + 2c_p & -2c_p \\ -2c_p & 2c_p \end{array} \right] \left\{ \begin{array}{c} \Omega_t \\ \Omega_v \end{array} \right\}, \tag{31.73}$$

$$\mathcal{T} = \frac{1}{2} \Omega_t^2 J_{tot} + \frac{1}{2} \Omega_v^2 J_v \tag{31.74}$$

and the equation of motion is simply

$$\left[\begin{array}{cc} J_{tot} & 0 \\ 0 & J_v \end{array} \right] \left\{ \begin{array}{c} \dot{\Omega}_t \\ \dot{\Omega}_v \end{array} \right\} + \left[\begin{array}{cc} \sum_{i=1}^{n-1} c_{1i} + 2c_p & -2c_p \\ -2c_p & 2c_p \end{array} \right] \left\{ \begin{array}{c} \Omega_t \\ \Omega_v \end{array} \right\} = \left\{ \begin{array}{c} M_m \\ M_v \end{array} \right\}. \tag{31.75}$$

M_m is the total driving torque, or better the constant component of the total driving torque.

Remark 31.9 This result is trivial, and could be obtained from the previous, simpler, models.

31.6.3 Torsional Dynamics of the Engine and Driveline

The following assumptions can be made in the study of torsional dynamics:

- The average speed of the engine and the vehicle are known functions of time;
- The changes in the average speeds are slow enough to neglect the derivatives of the average speeds with respect to time.

The derivative of the kinetic energy with respect to the ith generalized velocity is

$$\frac{\partial \mathcal{T}}{\partial \dot{\phi}_i} = \left[J_{0i} + J_{1i}\left(\theta_i\right)\right]\left(\Omega_t + \dot{\phi}_i\right) \ , \tag{31.76}$$

for $i = 1, ..., n-1$ and

$$\frac{\partial \mathcal{T}}{\partial \dot{\phi}_n} = J_{0n}\left(\Omega_v + \dot{\phi}_n\right) \ . \tag{31.77}$$

Differentiating with respect to time, it follows that

$$\frac{d}{dt}\left(\frac{\partial \mathcal{T}}{\partial \dot{\phi}_i}\right) = \left[J_{0i} + J_{1i}\left(\theta_i\right)\right]\ddot{\phi}_i + \frac{\partial J_{1i}\left(\theta_i\right)}{\partial t}\left(\Omega_t + \dot{\phi}_i\right) \ , \tag{31.78}$$

i.e.

$$\frac{d}{dt}\left(\frac{\partial \mathcal{T}}{\partial \dot{\phi}_i}\right) = \left[J_{0i} + J_{1i}\left(\theta_i\right)\right]\ddot{\phi}_i + \frac{\partial J_{1i}\left(\theta_i\right)}{\partial \theta_i}\left(\Omega_t + \dot{\phi}_i\right)^2 \ , \tag{31.79}$$

for $i = 1, ..., n-1$ and

$$\frac{d}{dt}\left(\frac{\partial \mathcal{T}}{\partial \dot{\phi}_n}\right) = J_{0n}\ddot{\phi}_n \ . \tag{31.80}$$

Finally, the derivatives of the kinetic energy with respect to the generalized coordinates are

$$\frac{\partial \mathcal{T}}{\partial \phi_i} = \frac{1}{2}\frac{\partial J_{1i}\left(\theta_i\right)}{\partial \theta_i}\left(\Omega_t + \dot{\phi}_i\right)^2 \ , \tag{31.81}$$

for $i = 1, ..., n-1$ and

$$\frac{\partial \mathcal{T}}{\partial \phi_n} = 0 \ . \tag{31.82}$$

Remembering that $J_{1i}(\theta_i)$ vanishes in the last equation of motion (it actually vanishes in all equations regarding nodes where no crank is located), the inertial part of all equations of motion is

$$\frac{d}{dt}\left(\frac{\partial \mathcal{T}}{\partial \dot{\phi}_i}\right) - \frac{\partial \mathcal{T}}{\partial \phi_i} = \left[J_{0i} + J_{1i}(\theta_i)\right]\ddot{\phi}_i + \frac{1}{2}\frac{\partial J_{1i}(\theta_i)}{\partial \theta_i}\left(\Omega_t + \dot{\phi}_i\right)^2 , \tag{31.83}$$

while in the last equation only the term $J_{0n}\ddot{\phi}_n$ is present.

The other terms of the equations of motion are

$$\left\{\frac{\partial \mathcal{U}}{\partial \phi_i}\right\} = \mathbf{K}\boldsymbol{\phi}, \tag{31.84}$$

$$\frac{\partial \mathcal{F}}{\partial \dot{\phi}_i} = \mathbf{C}\dot{\boldsymbol{\phi}} + (\mathbf{C}_1 + \mathbf{C}_3)\left\{\begin{array}{c}\Omega_t \mathbf{S}\\ \Omega_v\end{array}\right\} . \tag{31.85}$$

The final form of the equation of motion is then

$$\begin{aligned}\left[\mathbf{M}_0 + \mathbf{M}_1(\mathbf{x})\right]\ddot{\boldsymbol{\phi}} + \frac{1}{2}\frac{\partial \mathbf{M}_1(\mathbf{x})}{\partial \mathbf{x}}\left\{\left(\Omega_t + \dot{\phi}_i\right)^2\right\} + \\ + \mathbf{C}\dot{\boldsymbol{\phi}} + K\boldsymbol{\phi} = F - (\mathbf{C}_1 + \mathbf{C}_3)\left\{\begin{array}{c}\Omega_t \mathbf{S}\\ \Omega_v\end{array}\right\} ,\end{aligned} \tag{31.86}$$

where vector $\mathbf{F}$ contains the driving torques applied to the various cranks and the drag torque applied to the flywheel simulating the vehicle.

31.6.4 Traditional Approach

Not only does Eq. (31.86) contain coefficients that are varying in time, (through term θ_0 included in the total rotations $\mathbf{x}$ and then in $\mathbf{M}_1(\mathbf{x})$), but it is also nonlinear, both because ϕ_i are present in the total rotations $\mathbf{x}$ and then in $\mathbf{M}_1(\mathbf{x})$), and because it includes the squares of the generalized displacements ϕ_i.

The traditional approach is based on the following simplifications:

- $\mathbf{M}_1(\mathbf{x})$ is neglected with respect to $\mathbf{M}_0$ in the term in $\ddot{\boldsymbol{\phi}}$,
- $\dot{\phi}_i$ is neglected with respect to Ω_t in the term in $\left(\Omega_t + \dot{\phi}_i\right)^2$,
- $\mathbf{M}_1(\mathbf{x})$ is considered as a function of θ_0 but not of ϕ_i: The inertia of the crank system is considered as a function of the average rotation of the crankshaft, but not of the torsional rotation of the various cranks,
- usually, even if it is not strictly needed, the angular velocity Ω_t is assumed to be constant, and then $\theta_0 = \Omega_t t$.

In these conditions, the term

$$\frac{\partial \mathbf{M}_1(\mathbf{x})}{\partial \mathbf{x}} \left\{ \left(\Omega_t + \dot{\phi}_i\right)^2 \right\}$$

becomes a known function of time and then is brought to the right-hand side of the equation, together with the forcing functions.

The equation of motion reduces to

$$\mathbf{M}_0 \ddot{\phi} + \mathbf{C}\dot{\phi} + K\phi = \mathbf{F} + \mathbf{F}_{in} + (\mathbf{C}_1 + \mathbf{C}_3) \begin{Bmatrix} \Omega_t \mathbf{S} \\ \Omega_v \end{Bmatrix} , \tag{31.87}$$

where the terms

$$\mathbf{F}_{in} = -\frac{1}{2}\Omega_t^2 \frac{\partial \mathbf{M}_1(\theta_0)}{\partial \theta_0} \mathbf{S} \tag{31.88}$$

are usually defined as *inertia torques* of the cranks. By introducing the value of $\mathbf{M}_1$ in the equation, the various inertia torques are

$$\mathbf{F}_{in_i} = -\frac{1}{2}\Omega_t^2 \sum_{k=1}^{m} k \left[-J_{cik} \sin(k\theta_0 + \delta_{ik}) + J_{sik} \cos(k\theta_0 + \delta_{ik}) \right] . \tag{31.89}$$

Vector $\mathbf{F}$ contains the driving torque, which is periodic with period equal to the time needed to perform two revolutions of the crankshaft in a four-stroke cycle engine (fundamental frequency $\Omega_t/2$). $\mathbf{F}_{in}$ is also periodic, but its fundamental frequency is Ω_t. Usually, $\mathbf{F}_{in}$ is written as if its fundamental frequency were $\Omega_t/2$, with the amplitudes of all odd harmonics, including the fundamental one, set to zero. In this way the sum $\mathbf{F} + \mathbf{F}_{in}$ has a simpler structure.

The homogeneous equation associated with Eq. (31.87) does not take into account the variability in time of the equivalent moments of inertia of the crank systems. The natural frequencies are thus those of a system with constant inertia.

31.6.5 Numerical Approach

Equation (31.86) may be solved directly by numerical integration. If nonlinearity, and above all the dependence of the various parameters upon time, may make it difficult to proceed with the integration, the number of degrees of freedom of the system is nonetheless low (usually no more than 20), so the computation is not difficult. The time histories of the rotations of the various nodes can thus be obtained along with those of the stresses in the various parts of the crankshaft and driveline. The time histories can then be developed in Fourier series and the various harmonic contents extracted. However, if the time histories of the motion of the various elements of the driveline must be obtained, it now seems more expedient to resort directly to multibody computer codes instead of writing the equations of motion of the driveline and building *ad hoc* programs.

31.7 Multibody Driveline Models

The linearized models seen in the previous section have the advantage of yielding closed form, frequency domain solutions and of correctly simulating manoeuvres like tip-in, tip-out in a simple way. However, the assumption that the stiffness and damping characteristics of elements such as the clutch damper springs or elastomeric dampers may be simulated as linear springs and viscous dampers leads to a poor approximation.

The torsional characteristic of a clutch plate with damper springs is shown in Fig. 31.12a: Not only is it possible to identify three fields where the stiffness takes different values, but a well-defined hysteresis that has the characteristics of a dry friction is also present. The fact that the stiffness is variable in the three ranges does not prevent the elastic behavior about a particular working condition from being linearized, while the nature of the damping, which may be dealt with as dry friction, makes it impossible to linearize the behavior of this element if damping is accounted for. As an example, the hysteresis cycle for displacements about a condition in which the driving torque is 50 Nm is shown in Fig. 31.12b.

If a torsional displacement-torque characteristic like that shown in Fig. 31.12 prevents the use of linearized models, or better, introduces large errors if a linearization is attempted, it may be included without difficulty in a multibody model . Multibody codes operate by numerically integrating in time the nonlinear equations of motion and thus are ideal for cases like this. It is then possible to include the detailed mathematical models of nonlinear elements and proceed to simulate the behavior of the

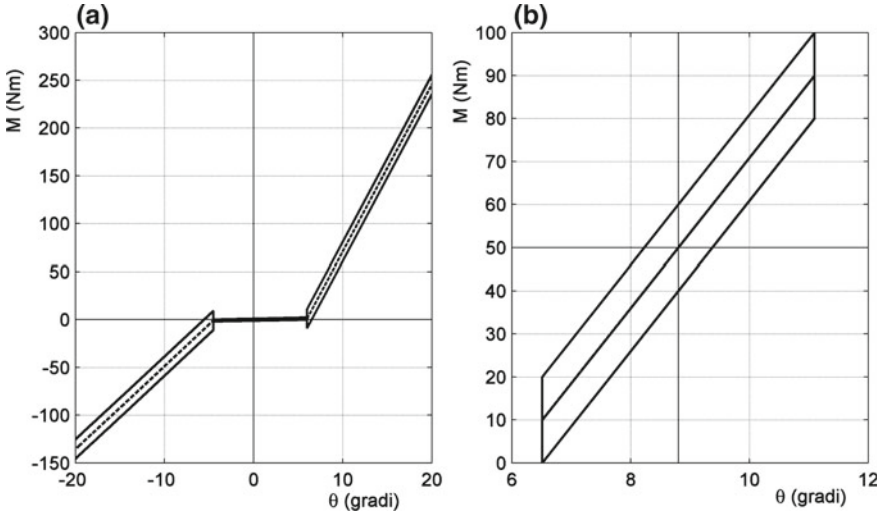

Fig. 31.12 Angular displacement-torque characteristics of a clutch with damper springs. **a** Characteristics with engine braking (left) and driving (right); **b** zoom on the zone of the plot for a condition where the torque cycles about a value of the driving torque of 50 Nm

driveline in detail. The engine may be modelled directly with the pistons, connecting rods and cranks, while its elastic supports may also be included. On the other end of the driveline, the suspension connecting the wheel to the vehicle body may also be included in the model with its compliance in the longitudinal direction, which often introduces a coupling between longitudinal motion of the vehicle and ride comfort. Multibody models may also include the engine control to correctly simulate various manoeuvres.

In the case of models restricted to the engine, multibody models that take the actual geometry of the reciprocating and rotating elements into account are increasingly replacing the traditional approach based on the modelling of the inertia torques applied to the cranks as external forcing functions. Obviously, their basic drawback of not allowing closed form solutions to be reached remains.